INFLUENCE OF SINTERING ATMOSPHERER ON THE MAGNETORESISTIVE PROPERTIES OF SCREEN PRINTED $La_{0.67}Ca_{0.33}MnO_3$ THICK FILMS

A. K. M. Akther Hossain*
Department of Physics, Bangladesh University of Engineering & Technology,
Dhaka 1000, Bangladesh.

Abstract Thick films of $La_{0.67}Ca_{0.33}MnO_3$ were fabricated on single crystal (100) $LaAlO_3$ (LAO), single crystal (100) yttria stabilised zirconia (YSZ) and polycrystalline alumina substrates by a screen printing technique. The films were sintered at 1400°C in air, oxygen and nitrogen atmospheres to explore the influence of the sintering atmosphere on the electrical transport and magnetoresistive properties. The thick films fabricated on Al_2O_3 substrates reacted very badly for the films sintered 1400°C in all atmospheres and are not suitable for further investigations. All films under investigation except film on YSZ substrate sintered at nitrogen atmosphere exhibit a metal-insulator (*M-I*) transition at so called peak temperature, T_{p1}. The T_{p1} varies from 187 to 265 K for various films of $La_{0.67}Ca_{0.33}MnO_3$, depending on substrates and sintering atmosphere. The thick film on LAO substrate sintered at 1400°C in oxygen shows 70% *MR* at 8 T near T_{p1} (230 K), whereas the thick film on YSZ substrate exhibits highest (94%) *MR* around T_{p1} (187 K) in an 8 T applied field. Besides this peak *MR* these films also show low temperature *MR*. Low temperature *MR* as a function of applied field, *MR(H)*, showed two slopes. A model was proposed to explain low temperature *MR(H)*.

Keywords: Colossal magnetoresistance, Thick film, Transition temperature, Screen printing

INTRODUCTION

The discovery of colossal magnetoresistive (CMR) effects in the mixed valent manganese perovskites have attracted much interest due to the importance of their potentia[1]l technological applications [Jin et al., 1994; Hwang et al., 1995; Rao et al., 1996; Ramirez, 1997]. Generally, CMR effect is observed in $R_{1-x}A_xMnO_3$ for $0.2<x<0.5$, where R is any trivalent rare earth material (La, Y, Pr etc) and A is divalent material (Ca, Sr, Ba etc). These materials exhibit a metal-insulator (*M-I*) transition accompanied by ferromagnetic-paramagnetic transition within a temperature range 100-400 K, depending on the composition, the dopant used and oxygen content [Jonker and Santen, 1950; Urushibara et al., 1995; Hwang et al., 1995; Schiffer et al., 1995; Hwang et al., 1996; Hundley et al., 1996; Ramirez, 1997]. The partial substitution of trivalent R^{3+} by divalent A^{2+} in $R_{1-x}A_xMnO_3$ system introduces a mixture of Mn^{3+} and Mn^{4+} ions. Both Mn ions have three electrons in the t_{2g} state forming a localised spin $S=3/2$, and Mn^{3+} has one extra electron in the e_g state, which can hop between nearest neighbour Mn ions via oxygen. The magnetic and electronic properties of mixed valent manganites arise from the strong coupling between these itinerant e_g electron and the localised spins [Zener, 1951; Anderson and Hasegawa, 1955]. For applications of manganite materials, we need to make the technology simple and cheap. The thick film offers a good opportunity for future magnetic sensor and read head applications. For this reason we are motivated to make manganite thick films by a screen printing technique on different substrates. The substrates play an important role in the properties of materials. We fabricated thick films of $La_{0.67}Ca_{0.33}MnO_3$ on both polycrystalline and single crystal substrates.

EXPERIMENTAL METHODS

The $La_{0.67}Ca_{0.33}MnO_3$ composition was synthesised using a conventional solid state reaction technique. High purity powders of La_2O_3 (Aldrich 99.99%), $CaCO_3$ (BDH 99.9%) and $MnCO_3$ (Aldrich 99.9$^+$%) were used to make the required composition. We pre-heat treated the La_2O_3 powder at 1000°C for 6 h before mixing with the other ingredients, as this is a hygroscopic chemical. The ingredients were weighed with appropriate proportions and then dry ball milled for 24 h. The calcination was done in 4 steps. The mixed powders were calcined at 950°C for 6 h, the temperature ramps being 300°C/h in both warming and cooling. This step was repeated three more times with intermediate grindings to obtain a homogeneous and phase pure composition. After a total period of 24 h of calcination, the final product was ultrasonically dispersed in water media to create powders of fine particle size. The dried fine powders were mixed with Blythe vehicle (Cookson

*Email: ahossain@phy.buet.edu

Matthey) to obtain ink. From this ink thick films were fabricated onto different substrates by screen printing. The screen printed thick films were kept in a desiccator over night to settle, and then the organic vehicle burnt out. The burning out of the organic vehicle was done at 300°C for 3 h and the temperature ramp was 30°C/h in both warming and cooling. Thick films were sintered at 1400°C in air, oxygen and nitrogen atmospheres for 1h. To check for the reproducibility in sintering behaviour some screen printed thick films were sintered under same conditions but in separate sintering runs.

The microstructures of the samples were investigated using a scanning electron microscope (SEM) (JEOL JSM-5300) with magnification ranging 750 up to 5000×. Images were acquired and analysed using image Tool 2.1 software. The thickness of the films was measured using a Zyro optical interferometer near the film edge.

The X-ray diffraction was carried out in our samples using an X-ray diffractometer (PW 1710) operating at 40 kV and 40 mA with a Ni filter, using Cu-Kα radiation with wavelength of 1.54060 A°. A (111) plane cleaved silicon single crystal was used for calibration. The diffraction pattern was obtained by a step scanning technique from 10-90° in 2θ with a step size of 0.02° and a count time of 3s. Unit cell parameters were calculated using the non-linear least square refinement program, Unitcell.

The DC electrical resistance of the thick films were measured by the standard four-point probe technique with a temperature range 295-20K with a cooling rate of 1.5 K/minute. The electrical contacts were made on contact pads of the films using conductive silver paint. Offset voltages were subtracted by reversing the current. The resistivity was calculated from the simple geometrical relation $R=\rho l/A$. For magnetoresistance measurements the applied field was perpendicular to the current flow in the sample. The magnetoresistance was calculated using,

$$MR(\%) = -\frac{\rho(H=0)-\rho(H)}{\rho(H=0)}\times 100$$

The magnetisation measurements were made on the whole thick film sample using an OI-3001 vibrating sample magnetometer. The trivial diamagnetic signal for the LAO and YSZ substrates compared to magnetisation of the whole sample was not subtracted from the net magnetisation of the sample.

RESULTS

Material Characterisation

Microstructures- SEM pictures of thick films of nominal composition $La_{0.67}Ca_{0.33}MnO_3$ on single crystal (100) LAO, YSZ substrates sintered at 1400°C in oxygen and nitrogen flow are shown in Fig. 1 and 2, respectively. Films on LAO sintered at 1400°C in nitrogen flow are densely packed with a larger grain size compared to the film on same substrate sintered in an oxygen atmosphere at the same temperature. This result agrees well with the literature [Valenzuela, 1994]. The microstructure of the films on YSZ substrates indicated that the grain growth is larger than on LAO substrate. Again the film on YSZ substrate sintered at nitrogen atmosphere has larger grain size compared to film sintered in Oxygen atmosphere. The grains are densely packed for the film on LAO substrate compared to the films on YSZ substrate sintered at same atmospheres.

X-ray analysis- X-ray analysis was carried out on all thick films. It was found that all samples are single phase within the sensitivity of the X-ray measurements. The unit cell parameters and the volume of unit cell for all films are tabulated in Table 1.

Table 1: Lattice parameters and unit cell volume of the $La_{0.67}Ca_{0.33}MnO_3$ thick films on various substrates sintered at 1400°C in various atmospheres. The samples were sintered at the temperature indicated for 1h.

Substrates	Sintering Atmo-spheres	Lattice parameters (Å)	Unit cell volume ($Å^3$)
LAO	Air	7.72	460.57
LAO	O_2	7.71	458.18
LAO	N_2	7.72	459.83
YSZ	Air	7.72	460.77
YSZ	O_2	7.72	460.47
YSZ	N_2	7.77	469.71

From Table 1, it was observed that the cubic lattice parameter is the smallest for the films sintered in oxygen atmospheres for both substrates. This is because the oxygenation of thick films creates more Mn^{4+}, which has a smaller ionic size compared to Mn^{3+} [Shannon, 1976]. This result agrees well with those reported earlier [Pierre et al., 1996; Ghivelder et al., 1998]. The thick film on YSZ substrate which was sintered in a nitrogen flow has the largest lattice parameters, which is the consequence of a drastic decrease of Mn^{4+} content.

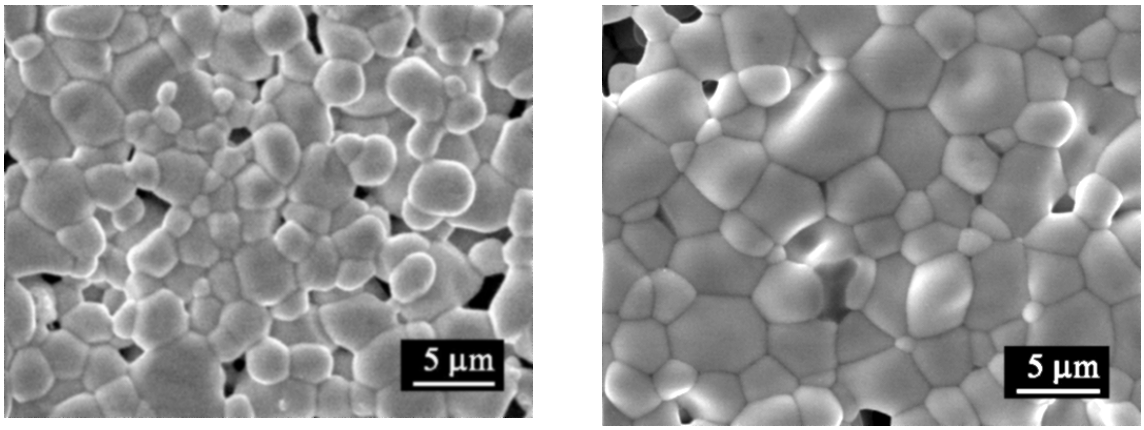

(a) **(b)**

Fig. 1 (a) SEM picture of thick film of $La_{0.67}Ca_{0.33}MnO_3$ on LAO substrate sintered at 1400°C in Oxygen flow (b) SEM picture of thick film of $La_{0.67}Ca_{0.33}MnO_3$ on LAO substrate sintered at 1400°C in Nitrogen flow

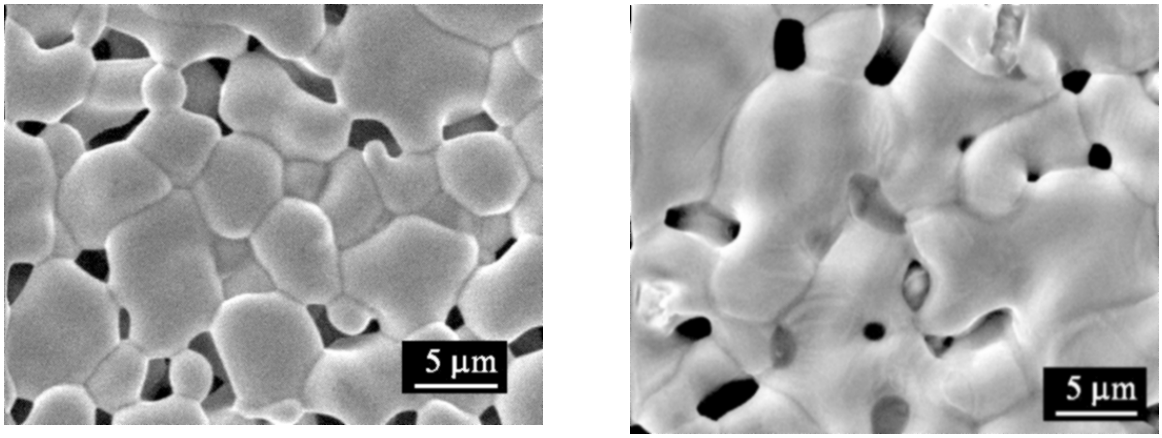

(a) **(b)**

Fig. 2 (a) SEM picture of thick film of $La_{0.67}Ca_{0.33}MnO_3$ on YSZ substrate sintered at 1400°C in Oxygen flow (b) SEM picture of thick film of $La_{0.67}Ca_{0.33}MnO_3$ on YSZ substrate sintered at 1400°C in Nitrogen flow.

Physical Properties of $La_{0.67}Ca_{0.33}MnO_3$ Films

DC Electrical Resistivity- The temperature dependence of the normalised resistivity, $\rho(T)/\rho(RT)$, at zero field for the films deposited on single crystal (100) LAO substrates, sintered at 1400°C in various atmosphere are shown in Fig. 3a. All thick films on LAO substrates show a *M-I* transition at different peak temperatures T_{pl}. The T_{pl} values are given in Table 2. The thick films sintered at 1400°C in oxygen shows two peaks in the ρ-T curves, like the peaks observed in the bulk samples prepared from the powder from which the ink of the thick films were made (not shown). The bulk sample which was prepared from the thick film powder has a very broad *M-I* transition and double peaks in the ρ-T curve. The thick films that were sintered in oxygen also show double peaks but ρ is an order of magnitude higher than that of the fully oxygenated bulk sample [Hossain et al., 1999]. Most of the thick films on LAO substrates have very broad *M-I* transitions at T_{pl} similar to the bulk samples prepared from the thick film powder. The T_{pl} varies from 250 to 258K for the thick films on LAO substrates. The highest T_{pl} was obtained for the film sintered at 1400°C in oxygen and this sample also has the lowest resistivity throughout the whole temperature range (295-20K). The ρ above T_{pl} follows an activated behavior $\rho(T) \propto exp\ (E_A/k_BT)$ for all samples. The activation energies (E_A) are given in Table 2.

The origin of different behaviour of ρ-T in the present composition might be due to the fact that it was prepared using a slightly deviated method. We pre-heated the La_2O_3 powder before mixing with the other ingredients. Usually, $La(OH)_3$ and $La_2O_2CO_3$ coexist within the commercial La_2O_3.To eliminate $La(OH)_3$ and $La_2O_2CO_3$, we heat treated the commercial La_2O_3 at 1000°C for 6 h and then cooled in a desiccator. Recently, Sun et al. [Sun et al., 1998] reported that nearly stoichiometric composition can be obtained when commercial La_2O_3 is used and purified La_2O_3 (heat-treated) results in oxygen deficiency.

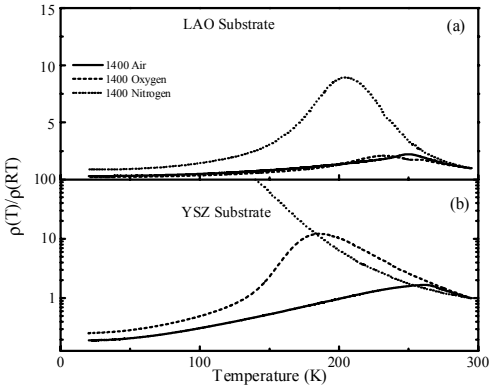

Fig. 3: Normalised zero field ρ as a function of temperature for the $La_{0.67}Ca_{0.33}MnO_3$ thick films (a) fabricated on single crystal (100) LAO substrates (b) single crystal (100) YSZ substrates. The sintering atmospheres are shown in figure

Fig. 3b shows the normalized ρ-T curves of the films fabricated on the single crystal (100) YSZ substrates for samples sintered at 1400°C. All films except the film sintered at 1400°C in nitrogen flow show a *M-I* transition at T_{p1}. The T_{p1} varies from 187-265K for the thick films on YSZ substrates. The film sintered at 1400°C in oxygen has the lowest T_{pl}. The ρ above T_{pl} follows an activated behaviour with a slight variation of activation energies. The T_{pl} values and the activation energies are given Table 2.

Table 2: The T_{p1}, thickness, activation energy and T_c of $La_{0.67}Ca_{0.33}MnO_3$ thick films on different substrates, where T_{p1} is the temperature correspond to the resistivity peak. T_c is the Curie-Weiss temperature and is taken from minimum in *dM/dT*.

Substrates	Atmo-sphere	Thickness (μm)	T_{p1} (K)	E_A (meV)	T_c (K)
LAO	Air	63.4	250	127	252
LAO	O_2	46.2	258	108	264
LAO	N_2	76.5	205	167	
YSZ	Air	42.9	263	116	263
YSZ	O_2	54.5	187	133	175
YSZ	N_2	58.7	-	110	167

Magnetoresistance-Magnetoresistance(*MR*) of samples were studied both as a function of temperature *MR(T)* at constant field, and *MR* as a function of field *MR(H)* at constant temperature. Fig. 4 shows *MR(T)* at 8T applied magnetic field for the film on YSZ substrate sintered at oxygen atmosphere. The *R(T)* curves in zero field and in presence of applied field for this sample are also shown in this figure. The maximum *MR* 94%, at T_{m1} (184 K) was obtained for this sample. Besides this, low temperature *MR* of 50% was obtained at 20 K with 8T applied field. Unlike the epitaxial and single crystal manganite samples the peak *MR* is not limited to a small temperature window, in fact a broad MR peak is obtained spanning a maximum 27 K. Also the low temperature *MR* is independent of temperature.

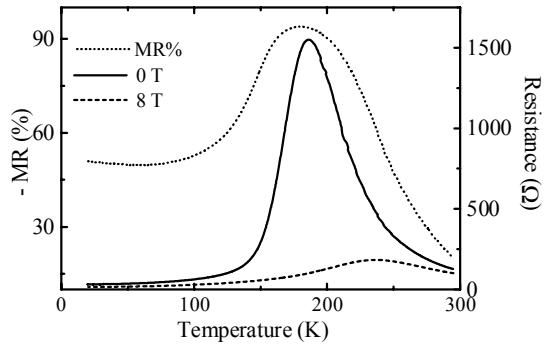

Fig. 4: Magnetoresistance as a function of temperature at 8 T field for the film on YSZ substrate sintered at oxygen atmosphere.

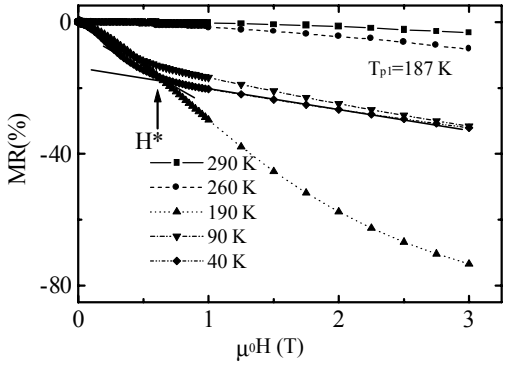

Fig. 5: Magnetoresistance as a function of field at various temperatures above and below T_{p1} for the film on YSZ substrate sintered at oxygen atmosphere

MR as a function of field at constant temperature for the film on YSZ substrate sintered at oxygen atmosphere is shown in Fig. 5. This graph indicates the *MR* sensitivities as a function of temperature and field. Like polycrystalline bulk samples [Hossain et al., 1999] this film also show two *MR* slopes at temperatures much below T_{p1} (e.g. 90 K and 40 K). The strong field dependence of *MR* exists for an applied field below H^* as shown in Fig 5. It was observed previously that H^* is a function of temperature and $H^*(T) \approx H_s(T)$ determined magnetically, where H_s is the saturation magnetising field [Hossain et al., 1999]. The low-temperature, low-field (below H^*) *MR* has been attributed to either spin-polarised tunnelling [Hwang et al., 1996], spin dependent scattering [Gupta et al., 1996; Mahesh et al., 1996; Li et al., 1997] or micromagnetic behaviour associated with alignment of magnetic domain at the grain boundaries [Eveits et al., 1998]. The origin of low-temperature, high field (above H^*) *MR* might be due to

the disordered or canted spin in the grain boundary region.

The observed two slopes MR at low temperature can be explain with the help of grain and grain boundary model as shown in Fig. 6. At $T<<T_c$ (where T_c is the paramagnetic to ferromagnetic transition temperature, which is close to the T_{p1}) the material is in the ferromagnetic state. However, in the absence of field the magnetisation of the grain of the polycrystalline material will be randomly aligned (Fig. 6a). Also the individual spins at the grain boundary region will be disordered. In the absence of field an electron will be suffer scattering from the non-aligned magnetic domain, as well as disordered spin at the grain boundary region. As a result of low applied magnetic field, the magnetisation of each grain starts to align towards the direction of the external magnetic field as shown in Fig. 6b. However, a large magnetic field is required to align the spins of the grain boundaries as shown in Fig. 6c.

Magnetic Properties of Thick Films - Fig. 7 shows *M-T* curves for various thick films sintered at 1400°C in various atmospheres. This data was taken in presence of remnant field of the magnet (~30 mT). All thick films show a paramagnetic to ferromagnetic transition at T_c. The T_c*s* are defined by the minima in *dM/dT* and the values are given in Table 2. It was observed that the T_c*s* are very close to T_{p1} measured from resistivity. However, the film on YSZ substrate sintered at nitrogen atmosphere has a T_c ~167 K but no T_{p1} was observed in $\rho(T)$ curve.

Reproducibility of the Thick Films – To check the reproducibility of thick films properties some films were sintered in oxygen atmospheres in a separate sintering run. It was observed that the transport properties and magnetoresistive properties are very similar. From this random reproducibility check it was concluded that properties of thick films are reproducible.

CONCLUSIONS

We have fabricated manganite thick films on various substrates using a screen printing technique. The screen printing has proven to be successful technique for the preparation of high quality reproducible thick films. We have observed a wide variation of T_{p1} for the thick films on different substrates sintered at different atmospheres. This variation is due to the influence of substrates and different oxygen partial pressures in sintering as the growth conditions are important for the manganite thick films.

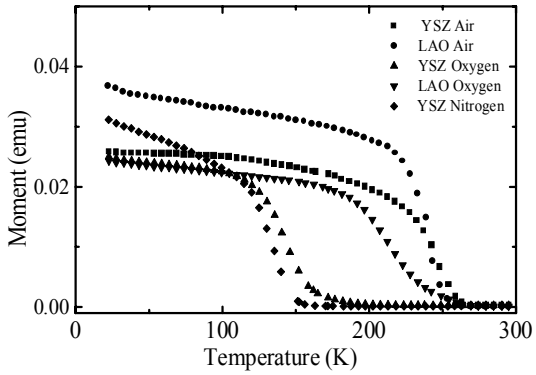

Fig. 7: Magnetic Moment as a function of temperature for the films on various substrates sintered at 1400°C in various atmospheres

The physical properties of the thick films are either similar or show improve MR properties compared to bulk polycrystalline samples prepared from the same powders. The highest MR obtained for the thick films is 94% in 8 T applied field near T_{p1} for 1400°C in oxygen on YSZ. Besides this, a low-temperature MR of 50% has been obtained at 20K for this film. For some films this low-temperature MR is temperature independent.

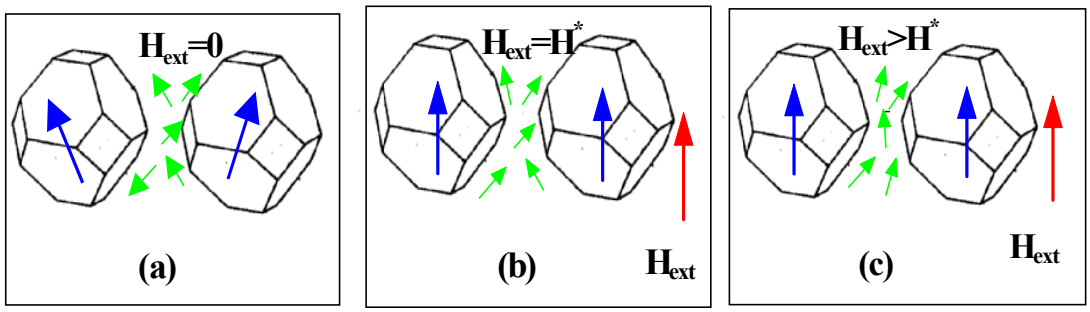

Fig. 6 Grain and grain boundary model for explaining the observed two slopes *MR* at low-temperature ($T<<T_{p1}$) in polycrystalline thick films (a) zero applied field $H_{ext}=0$, (b) $H_{ext}=H^*$ and (c) $H_{ext}>H^*$. We assumed tetrakaidecahedral (truncated octahedral) grain shape

The films show CMR near T_{p1} and also low temperature *MR*. The low temperature *MR* exhibits two slopes. Highly sensitive low-temperature low-field *MR* persists up to certain applied field H^*. At low temperature, two slopes *MR* is explained with the help of grain and grain boundary model. Highly sensitive low temperature and low field *MR* is due to the grain boundary. This sensitive grain boundary related *MR* found in the polycrystalline thick film may be very useful for practical applications.

ACKNOWLEDGEMENTS

Author would like to thank Association of Commonwealth Universities for the scholarship tenable at Imperial College, London. Author also would like to thank Dr. L. F. Cohen and Dr. J. Driscoll of Imperial College, London, allowing him to use their Laboratory Facilities.

REFERENCES

Anderson P. W. and Hasegawa, H. "Consideration on Double Exchange", *Phys. Rev.,* **100**(2), 675-681 (1955).

Evetts, J. E. Blamire, M. G. et al. "Defect-induced spin disorder and magnetoresistance in single-crystal and polycrystal rare earth manganite thin films", *Phil. Trans. R. Soc. Lond. A,* **356**, 1593-1615 (1998).

Ghivelder, L. Abrego Castillo, I. et al. "Specific Heat of $La_{1-x}Ca_xMnO_{3-\square}$", *J. Magn. Magn. Mater.,* **189**(3), 274-282 (1998).

Gupta, A. Gong, G. Q. et al. "Grain-boundary effects on the magnetoresistance properties of perovskite manganite films", *Phys. Rev. B,* **54**(22), R15629- 15632 (1996).

Hossain, A. K. M. Akther. Cohen, L. F. et al. "Influence of grain size on magnetoresistance properties of bulk $La_{0.67}Ca_{0.33}MnO_{3-\square}$", *J. Magn. Magn. Mater.,* **192**(2), 263-270 (1999).

Hossain, A. K. M. Akther. Cohen, L. F. et al. "Influence of oxygen vacancies on magnetoresistance properties of bulk $La_{0.67}Ca_{0.33}MnO_{3-\square}$", *J. Magn. Magn. Mater.,* **195**(1), 31-36 (1999).

Hundley, M. F. Neumeier, J. J. et al. "Transport and magnetism correlation in thin film ferromagnetic oxides", *J. Appl. Phys.,* **79**(8), 4535-4537 (1996).

Hwang, H. Y. Cheong, S. –W. et al. "Lattice effects on the magnetoresistance in doped $LaMnO_3$", *Phys. Rev. Lett.,* **75**(2), 914-917 (1995).

Hwang, H. Y. Cheong, S. –W. et al. "Spin Polarized Intergrain Tunnelling in $La_{2/3}Sr_{1/3}MnO_3$", *Phys. Rev. Lett.,* **77**(10), 2041-2044 (1996).

Jin, S. Tiefel, T. H. et al. "Thousandfold change in resistivity in magnetoresistive La-Ca-Mn-O films", *Science,* **264**, 413-415 (1994).

Jonker, G. H. and Santen, J. H. V. "Ferromagnetic Compounds of Manganese with Perovskite Structure", *Physica,* **XVI**(3), 337-349 (1950).

Li, X. W. Gupta, A. et al. "Low field magnetoresistive properties of ploycrystalline and epitaxial perovskite manganite films", *Appl. Phys. Lett.,* **71**(8), 1124-1126 (1997).

Mahesh, R. Mahendiran, R. et al. "Effect of particle size on the giant magnetoresistance of $La_{0.7}Ca_{0.3}MnO_3$", *Appl. Phys. Lett.,* **68**(16), 2291- 2293 (1996).

Pierre, J. Robaut, F. et al. "Semiconductor-metal transition and magnetoresistance in (La, Ca)MnO_3: Experiments and simple model", *Physica B,* **225**, 214-224 (1996).

Ramirez, A. P. "Colossal magnetoresistance", *J. Phys. Conden. Matt.,* **9**, 8171-8199 (1997).

Rao, C. N. R. Cheetham, A. K. et al. "Giant magnetoresistance and related properties of rare- earth manganites and other oxide systems", *Chem. Mater.,* **8**, 2421-2432 (1996).

Schiffer, P Ramirez, A. P et al. "Low Temperature Magnetoresistance and the Magnetic Phase Diagram of $La_{1-x}Ca_xMnO_3$", *Phys. Rev. Lett.,* **75**(18), 3336-3339 (1995).

Shannon, R. D. "Revised effective ionic radii and systematic studies of interatomic distances ain halides and chalcogenides", *Acta Cryst.,* **A32**, 751- 767 (1976).

Sun, J. R. Rao, G. H. et al. "Effects of inhomogenious oxygen content in (La, Gd)$_{0.7}Ca_{0.3}MnO_{3+\square}$ perovskites", *Appl. Phy. Lett.,* **72**(24), 3208-3210 (1998).

Urushibara, A. Moritomo, Y. et al. "Insulator metal transition and giant magnetoresistance in $La_{1-x}Sr_xMnO_3$", *Phys. Rev. B,* **51**(20), 14103-14109 (1995).

Valenzuela, R. "*Magnetic ceramics",*Cambridge University Press , Pages (1994).

Zener, C. "Interaction Between the d Shells in the Transition Metals", *Phys. Rev.,* **81**(4), 440-444 (1951). Zener, C. "Interaction between the d-shells in the transition metals. II. Ferromagnetic compounds of manganese with perovskite structure", *Phys. Rev.,* **82**(3), 403-405 (1951).